University of Saskatchewan
Subatomic Physics Internal Report

SPIR 150

Bethe-Heitler Measurable Asymmetry

Rob Pywell

October 19, 2016

Abstract

This report describes an investigation of the resolution we can expect for the measured asymmetry in the Bethe-Heitler pair-production experiment.

Contents

1 Introduction

We now have access to a robust `C++` code that can calculate the cross sections for the Bethe-Heitler pair production process. This is the cross section described in [3]. This has been kindly provided Sasha Milstein and Peter. Using this code I have been able to calculate the theoretical energy asymmetry directly from the cross sections. The intent is to include these cross sections into the Geant4 simulation code for the pair spectrometer [2] to investigate the resolution achievable by the experiment [1].

This report is divided into two steps. A first step is to use a simpler Monte-Carlo code to first confirm the operation of the cross-section code, and to get an idea of the possible measurable energy asymmetry without using the full Geant4 simulation. This code simulates the experiment using the cross section code and adds on the expected experimental uncertainties at the end. This avoids the difficulty of choosing initial events for the Geant4 simulation from a probability distribution defined by the cross section.

The second step is to generate events for input to the full Geant4 simulation of the spectrometer. The initial steps in that work is described in Section 7.

2 The Cross Section Code

The code as supplied makes use of look-up tables to significantly increase the speed of calculation over a code the mimics the operation of the parent `Mathematica` code. I have written a "wrapper" code that provides a `C++` class `BH_cross_sections` that simplifies the use of the code and insulates the internal global variables needed within the code from any code written by the user. This code is available at `nucleus.usask.ca`. When compiled this code provides a library `libBH_cross_sections.so` which may be included in any `C++` application.

For a given photon energy, E_γ, and target nucleus with atomic number Z, the BH cross section code can calculate both the symmetric $d\sigma_s(\boldsymbol{p},\boldsymbol{q})$ and anti-symmetric $d\sigma_a(\boldsymbol{p},\boldsymbol{q})$ parts of the cross section, where $\boldsymbol{p}$ and $\boldsymbol{q}$ are the momenta of the electron and positron respectively. The total differential cross section is

$$d\sigma(\boldsymbol{p},\boldsymbol{q}) = d\sigma_s(\boldsymbol{p},\boldsymbol{q}) + d\sigma_a(\boldsymbol{p},\boldsymbol{q}) \tag{1}$$

$$d\sigma_s(\boldsymbol{p},\boldsymbol{q}) = \frac{d\sigma(\boldsymbol{p},\boldsymbol{q}) + d\sigma(\boldsymbol{q},\boldsymbol{p})}{2} \tag{2}$$

$$d\sigma_a(\boldsymbol{p},\boldsymbol{q}) = \frac{d\sigma(\boldsymbol{p},\boldsymbol{q}) - d\sigma(\boldsymbol{q},\boldsymbol{p})}{2} \tag{3}$$

We can also write

$$d\sigma(\boldsymbol{p},\boldsymbol{q}) = d\sigma(\varepsilon_p,\varepsilon_q,\theta_p,\theta_q,\phi_q) \tag{4}$$

where ε_p and ε_q are the total energies of the electron and positron, θ_p and θ_q are the polar angles of the electron and positron, and ϕ_q is the azimuthal angle of the positron relative to the electron. These are the inputs used in the functions included in the `BH_cross_sections` library. An example of using the library functions is given below.

```
#include "BH_cross_sections.h"
  // Set up the calculation for a specific Z and e_gamma.
  BH_cross_sections * xs = new BH_cross_sections(Z, e_gamma);
  // e_gamma in MeV
  // full cross section
  double xsec = xs->xsec_full(e_p, e_q, th_p, th_q, phi_q);
  // e_p and e_q in MeV, th_p, th_q and phi_q in radians
  // symmetric part cross section
  double xsec = xs->xsec_s(e_p, e_q, th_p, th_q, phi_q);
  // anti-symmetric part cross section
  double xsec = xs->xsec_a(e_p, e_q, th_p, th_q, phi_q);
```

3 The Theoretical Asymmetry

Our experiment is aimed at measuring the *energy asymmetry* which is defined for the specific condition that the electron and positron emerge in the same plane as the incident photon and the polar angles of the electron and positron are the same. i.e. $\theta_p = \theta_q = \theta$ and $\phi_q = 180°$. We define $\delta = \varepsilon_p - \varepsilon_q$, then the energy asymmetry is

$$\epsilon(\delta, \theta) = \frac{N(\delta, \theta) - N(-\delta, \theta)}{N(\delta, \theta) + N(-\delta, \theta)} \tag{5}$$

where $N(\delta, \theta)$ are the number of events observed with the given conditions.

From the definition of the cross sections we see that

$$\epsilon(\delta, \theta) = \frac{d\sigma(\boldsymbol{p}, \boldsymbol{q}) - d\sigma(\boldsymbol{q}, \boldsymbol{p})}{d\sigma(\boldsymbol{p}, \boldsymbol{q}) + d\sigma(\boldsymbol{q}, \boldsymbol{p})} \tag{6}$$

We write

$$\begin{aligned} d\sigma(\delta, \theta) &= d\sigma(\boldsymbol{p}, \boldsymbol{q}) = d\sigma(\varepsilon_p, \varepsilon_q, \theta, \theta, \pi) \\ d\sigma(-\delta, \theta) &= d\sigma(\boldsymbol{q}, \boldsymbol{p}) = d\sigma(\varepsilon_q, \varepsilon_p, \theta, \theta, \pi) \end{aligned} \tag{7}$$

and we also note that

$$\begin{aligned} d\sigma(\delta, \theta) &= d\sigma_s(\delta, \theta) + d\sigma_a(\delta, \theta) \\ d\sigma_s(-\delta, \theta) &= d\sigma_s(\delta, \theta) \\ d\sigma_a(-\delta, \theta) &= -d\sigma_a(\delta, \theta) \end{aligned} \tag{8}$$

Therefore

$$\epsilon(\delta, \theta) = \frac{d\sigma_a(\delta, \theta)}{d\sigma_s(\delta, \theta)} \tag{9}$$

The theoretical energy asymmetry can be calculated using the following procedure. For a given E_γ and Z we choose various combinations of θ and δ. For a given combination of E_γ, θ and δ the values of ε_p and ε_q are fixed by the three-body kinematics that includes the

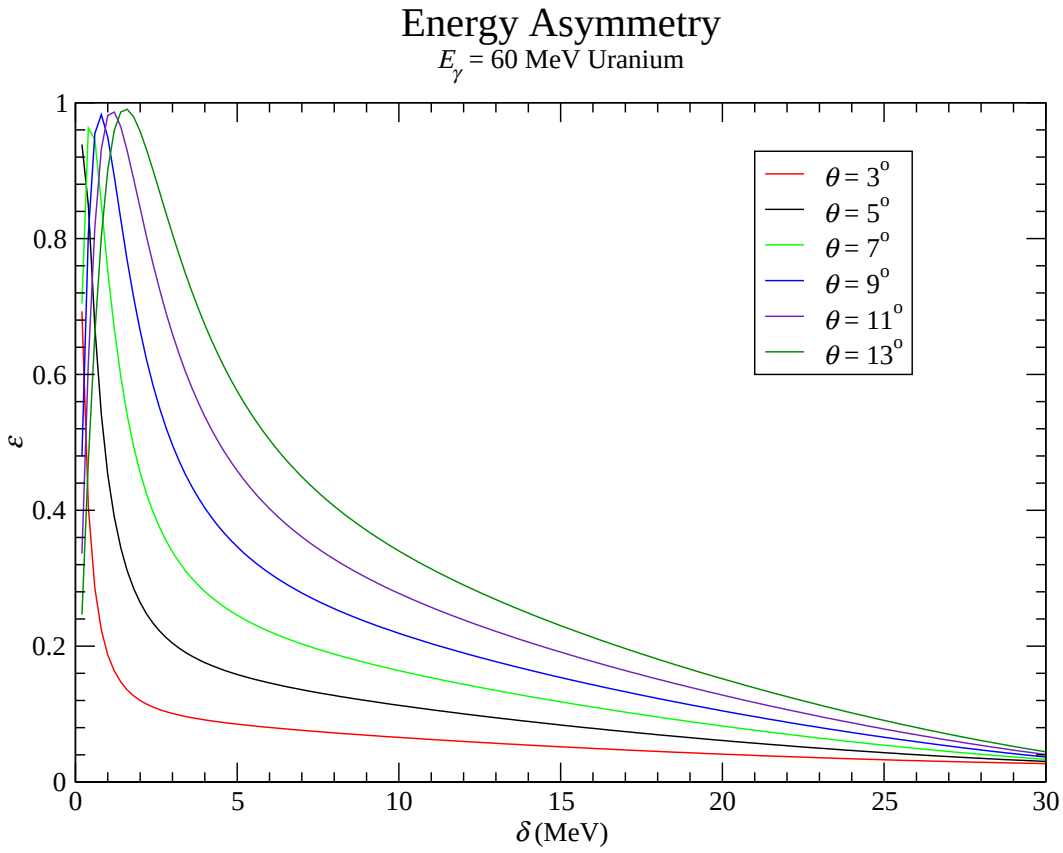

Figure 1: The theoretical energy asymmetry for 60 MeV photons on Uranium calculated as a function of δ for various values of the opening angle θ.

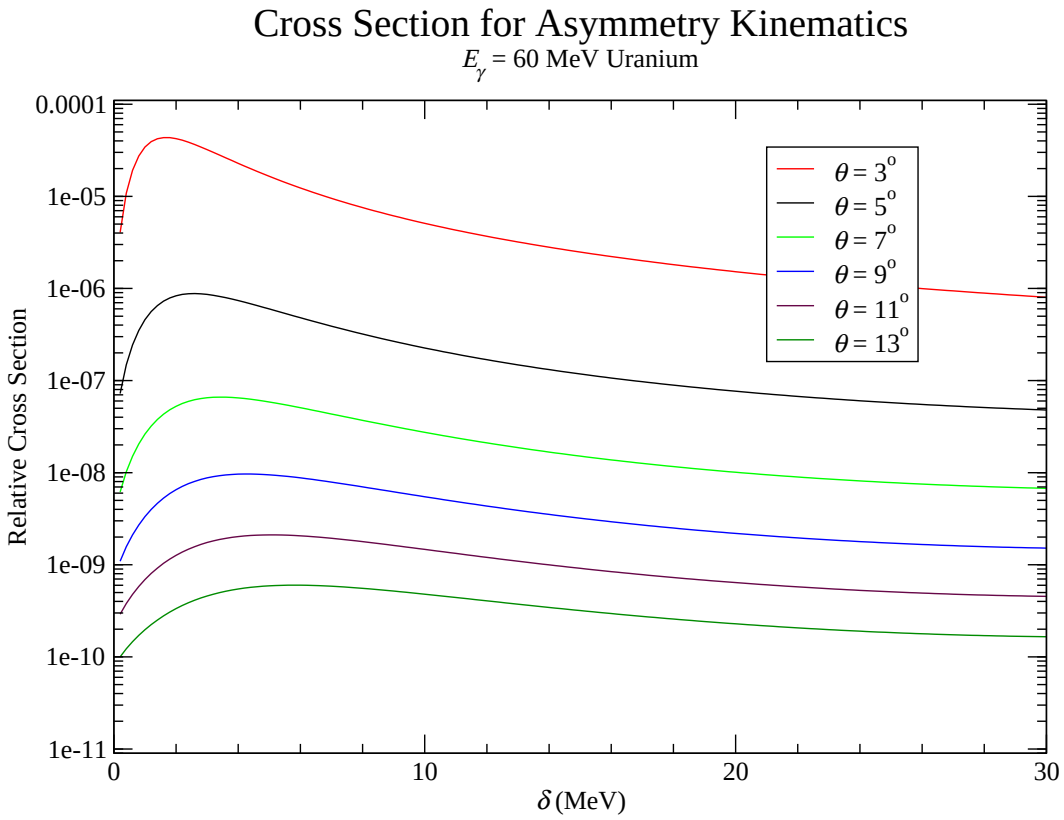

Figure 2: The relative differential cross sections for the same kinematic conditions as shown in figure 1.

recoil of the nucleus. (For our situation the recoil kinetic energy of the nucleus is is always found to be very small.) The asymmetry can then be calculated from (9). This asymmetry, calculated for Uranium with $E_\gamma = 60$ MeV, is shown in figure 1.

The relative differential cross section for the kinematic conditions required for the asymmetry shown in figure 1 is shown in figure 2. It can be seen the the cross section decreases rapidly with increasing polar angle θ, while at a particular θ the cross section changes relatively slowly with the energy difference δ.

4 The Experimental Asymmetry

In an experiment we do not have the luxury of choosing the polar angle θ and energy difference δ. Instead we measure all combinations of K_p, θ_p, ϕ_p, K_q, θ_q, and ϕ_q, that are within the acceptance of the spectrometer. Here K_p and K_q are the electron and positron kinetic energies ($K_p = \varepsilon_p - m_e$, $K_p = \varepsilon_p - m_e$, and m_e = electron mass).

Below I detail, rather pedantically, how we would sort these events to form a final measured asymmetry. I do this because it will be important for understanding the results of a Monte-Carlo simulation described in the following section.

Of course what we measure are quantities that are smeared by the finite resolution of the spectrometer. These resolutions may be characterized by standard deviations σ_K, σ_θ, and σ_ϕ. i.e. what we measure are;

$$\begin{aligned} K_{p,meas} &= K_p + G(\sigma_K) \\ K_{q,meas} &= K_q + G(\sigma_K) \\ \theta_{p,meas} &= \theta_p + G(\sigma_\theta) \\ \theta_{q,meas} &= \theta_q + G(\sigma_\theta) \\ \phi_{p,meas} &= \phi_p + G(\sigma_\phi) \\ \phi_{q,meas} &= \phi_q + G(\sigma_\phi) \end{aligned} \tag{10}$$

where K_p, θ_p, ϕ_p, K_q, θ_q, and ϕ_q are the actual quantities following the pair-production event withing the target, and the $G(\sigma)$ is Gaussian distribution centered on zero with standard deviation σ. Note: It is an assumption at this stage that the functions $G(\sigma)$ are symmetric Gaussian distributions. In the real spectrometer these distributions may turn out to be not Gaussian and not symmetric. Nevertheless the investigations using the Geant4 simulation of the spectrometer in SPIR-148[2] do suggest that that a Gaussian distribution is not a bad approximation.

We then choose only those events that satisfy our criteria for the kinematics required for the energy asymmetry. i.e. we impose the conditions:

$$\begin{aligned} |\theta_{p,meas} - \theta_{q,meas}| &< \Delta\theta_{tol} \\ ||\phi_{p,meas} - \phi_{q,meas}| - 180^\circ| &< \Delta\phi_{tol} \end{aligned} \tag{11}$$

Here $\Delta\theta_{tol}$ and $\Delta\phi_{tol}$ will be tolerances chosen to be commensurate with the resolutions of the spectrometer. For those events we form the quantities

$$\begin{aligned} \theta_{meas} &= (\theta_{p,meas} + \theta_{q,meas})/2 \\ \delta_{meas} &= K_{p,meas} - K_{q,meas} \end{aligned} \tag{12}$$

These are then accumulated in histograms. The histograms have finite bin widths. Therefore to be accepted into a bin the quantities must satisfy

$$\begin{aligned} |\theta_i - \theta_{meas}| &< \Delta\theta_{bin}/2 \\ |\delta_j - \delta_{meas}| &< \Delta\delta_{bin}/2 \end{aligned} \tag{13}$$

where θ_i and δ_j are the values at the center of histogram bins with bin widths $\Delta\theta_{bin}$ and $\Delta\delta_{bin}$.

Eventually we will end up with a number of counts $N[\theta_i][\delta_j]$ in a bin centered on θ_i and δ_j. Finally we can form the experimental asymmetry from

$$\epsilon_{meas}[\theta_i][\delta_j] = \frac{N[\theta_i][\delta_j] - N[\theta_i][-\delta_j]}{N[\theta_i][\delta_j] + N[\theta_i][-\delta_j]}. \tag{14}$$

5 Simple Monte-Carlo Simulation

A simulation of the expected experimental asymmetry using our Geant4 model for the pair spectrometer would begin by choosing an initial set of K_p, K_q, θ_p, θ_q, ϕ_p, and ϕ_q that are kinematically consistent and are chosen from a probability distribution defined by the differential cross section. The Geant4 simulation would then be used to find the experimental values $K_{p,meas}$, $K_{q,meas}$, $\theta_{p,meas}$, $\theta_{q,meas}$, $\phi_{p,meas}$, and $\phi_{q,meas}$ and the determination of the experimental asymmetry can follow as described in section 4. However, since the cross section varies over several orders of magnitude, the process of choosing an event to simulate will be very time consuming.

Therefore, as a first step, I wrote a simple Monte-Carlo simulation that mimics the determination of the experimental asymmetry described in section 4, but only needs to calculate the cross section in the final step after it has been determined in which histogram bins the event will fall. The simulation accumulates the information needed to determine the probability that an event will end up in a particular θ_i and δ_j bin.

The simulation proceeds as follows:
For each event:

1. Choose random values for K_p, θ_p, ϕ_p, θ_q, ϕ_q that populate phase space uniformly and are within (approximately) the acceptance of the spectrometer.

2. These values, along with the photon energy E_γ, then uniquely determine K_q.

3. These values are then smeared by the experimental resolutions that have been determined from the Geant4 simulation of the spectrometer. This step yields values of $K_{p,meas}$, K_{q_meas}, $\theta_{p,meas}$, $\theta_{q,meas}$, $\phi_{p,meas}$, and $\phi_{q,meas}$ (from Equation. (10)).

4. The event is rejected if it does not pass the asymmetry kinematic conditions requirement (Equation. (11)).

5. The event is rejected if it does not fall within one of the histogram bins (Equation. (13)).

6. The cross section for this event is calculated $d\sigma = d\sigma(K_p + m_e, K_q + m_e, \theta_p, \theta_q, \phi_q - \phi_p)$

7. The bin $N[\theta_i][\delta_j]$ is incremented. As well the sums $\sigma_{sum}[\theta_i][\delta_j]$ += $d\sigma$ and $\sigma^2_{sum}[\theta_i][\delta_j]$ += $d\sigma^2$ are incremented.

After a total number of events $N = \sum_{i,j} N[\theta_i][\delta_j]$ are accumulated, we calculate the average cross section for an event to end up in each bin.

$$\bar{\sigma}[\theta_i][\delta_j] = \frac{\sigma_{sum}[\theta_i][\delta_j]}{N[\theta_i][\delta_j]} \tag{15}$$

(Note that the sum $\sigma^2_{sum}[\theta_i][\delta_j]$ is used in the calculation of the uncertainty in $\bar{\sigma}$ as determined from the simulation; see Appendix A.)

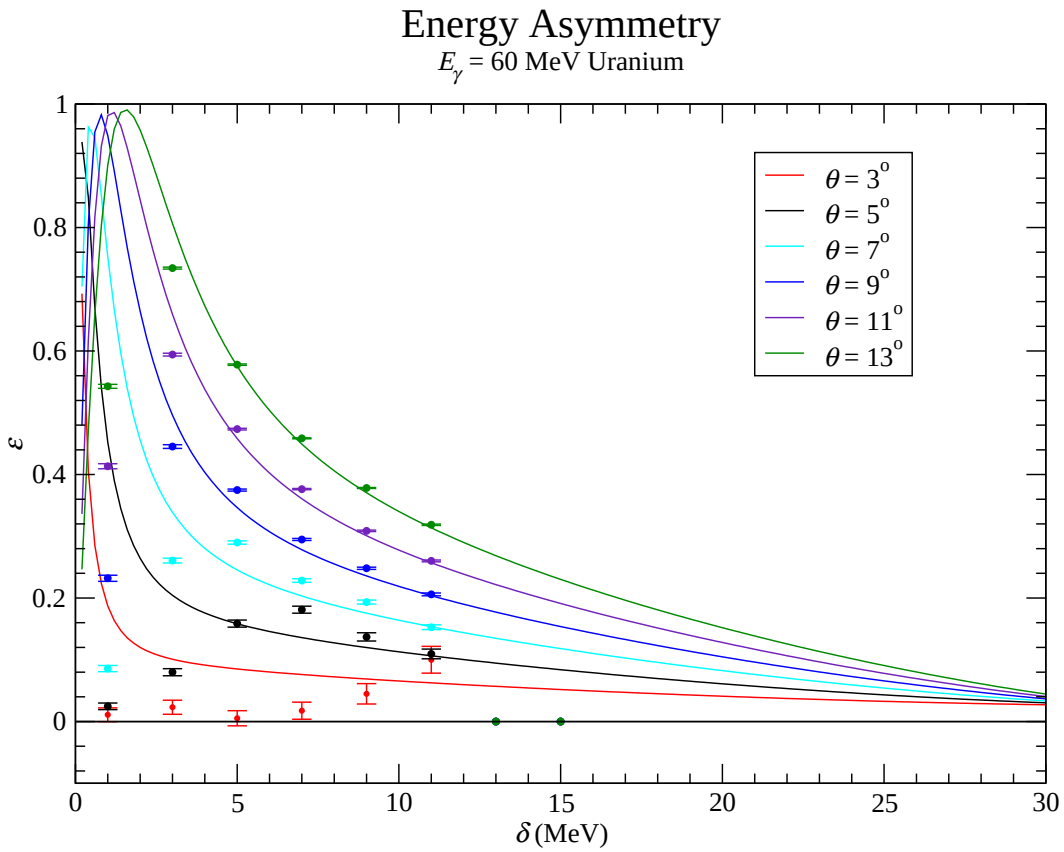

Figure 3: Measurable asymmetry with $\sigma_p = \sigma_q = \sigma_\theta = \sigma_\phi = 0$, $\Delta\theta_{tol} = 1°$, $\Delta\phi_{tol} = 1°$, $\Delta\theta_{bin} = 0.5°$ and $\Delta\delta_{bin} = 0.25$ MeV). 10^6 events that satisfied the criteria to fall within a bin were simulated.

6 Measurable Asymmetry

At this point we can calculate the measurable asymmetry given by the characteristics of the spectrometer and the need to bin the results.

The average cross section calculated in Equation. (15) will be proportional to the number of counts that will appear in the bin at θ_i and δ_j. Therefore the measurable asymmetry can be calculated from Equation. (14) by replacing $N[\theta_i][\delta_j]$ with $\bar{\sigma}[\theta_i][\delta_j]$.

As a first check that the code is working as expected we first calculate the measurable asymmetry with the spectrometer resolutions set to zero (i.e. $\sigma_p = \sigma_q = \sigma_\theta = \sigma_\phi = 0$). We also set the angular tolerances for events to satisfy the kinematics required by the energy asymmetry to be smaller than will be reasonable in the actual experiment (i.e. $\Delta\theta_{tol} = 1°$ and $\Delta\phi_{tol} = 1°$). As well we set the bin widths to small values to minimize any effect due to finite bin sizes (i.e. $\Delta\theta_{bin} = 0.5°$ and $\Delta\delta_{bin} = 0.25$ MeV). The result is shown in figure 3. It can be seen that we do reproduce the theoretical asymmetry except at smaller values of θ and δ where apparently the still finite bin widths are important.

Note: The error bars on the figures in this section do not represent expected experimental

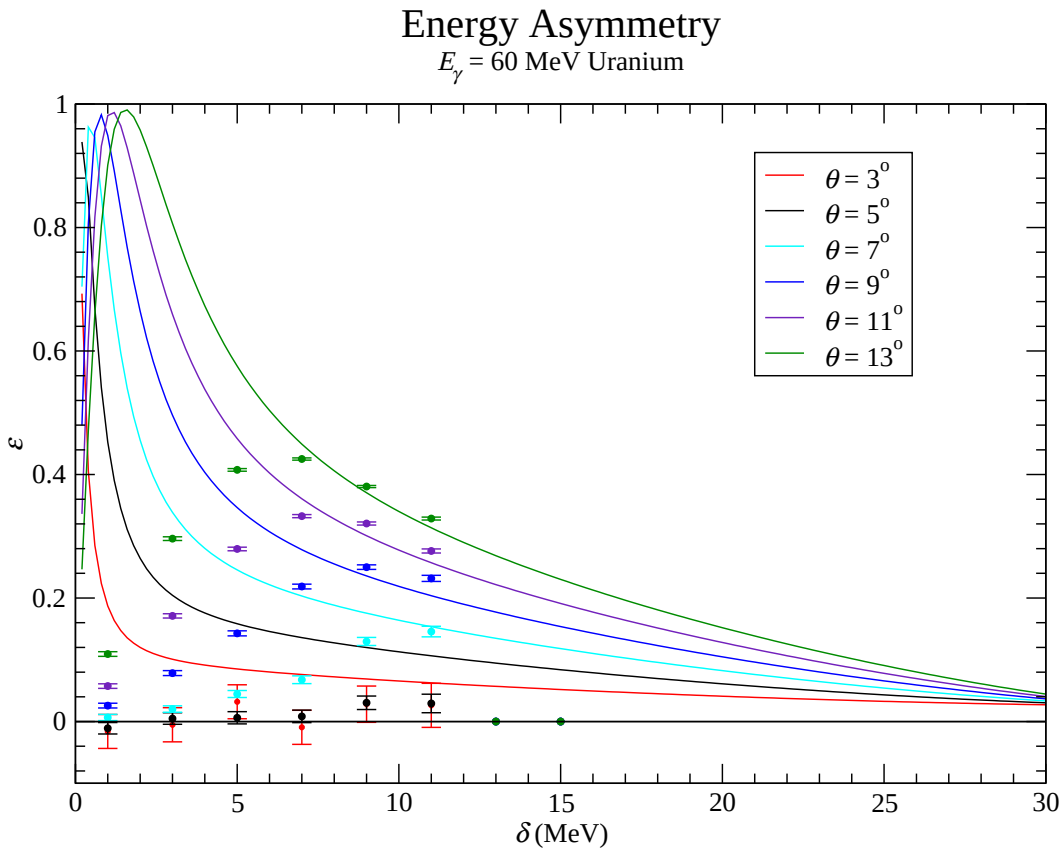

Figure 4: Measurable asymmetry with $\sigma_p = \sigma_q = \sigma_\theta = \sigma_\phi = 0$, $\Delta\theta_{tol} = 2.5°$, $\Delta\phi_{tol} = 8°$, $\Delta\theta_{bin} = 2°$ and $\Delta\delta_{bin} = 2$ MeV). 10^6 events that satisfied the criteria to fall within a bin were simulated.

uncertainties, but are only dependent on how long the Monte-Carlo simulation is run.

Next we set the bin widths to their correct values (i.e. $\Delta\theta_{bin} = 2.°$ and $\Delta\delta_{bin} = 2.$ MeV). As well we set the angular tolerances for events to satisfy the kinematics required by the energy asymmetry to be more reasonable values commensurate with the spectrometer resolution (i.e. $\Delta\theta_{tol} = 2.5°$ and $\Delta\phi_{tol} = 8°$). The result is shown in figure 4. It can be seen that at small polar angles $\theta < 7°$ the measurable asymmetry is essentially zero, while at larger polar angles and $\delta > 6$ MeV the measurable asymmetry is still close to the theoretical asymmetry.

Finally we include the effects of finite experimental resolution i.e. we set $\sigma_p = \sigma_q = 1.4$ MeV, $\sigma_\theta = 2.5°$ and $\sigma_\phi = 7.8°$. The result is shown in figure 5. In this Monte-Carlo run 10^8 events that fall within at least one bin were simulated. It can be seen that the finite experimental resolution has a very large effect on the measurable asymmetry. The measurable asymmetry for all polar angles $\theta < 11°$ is zero within the uncertainties of the simulation.

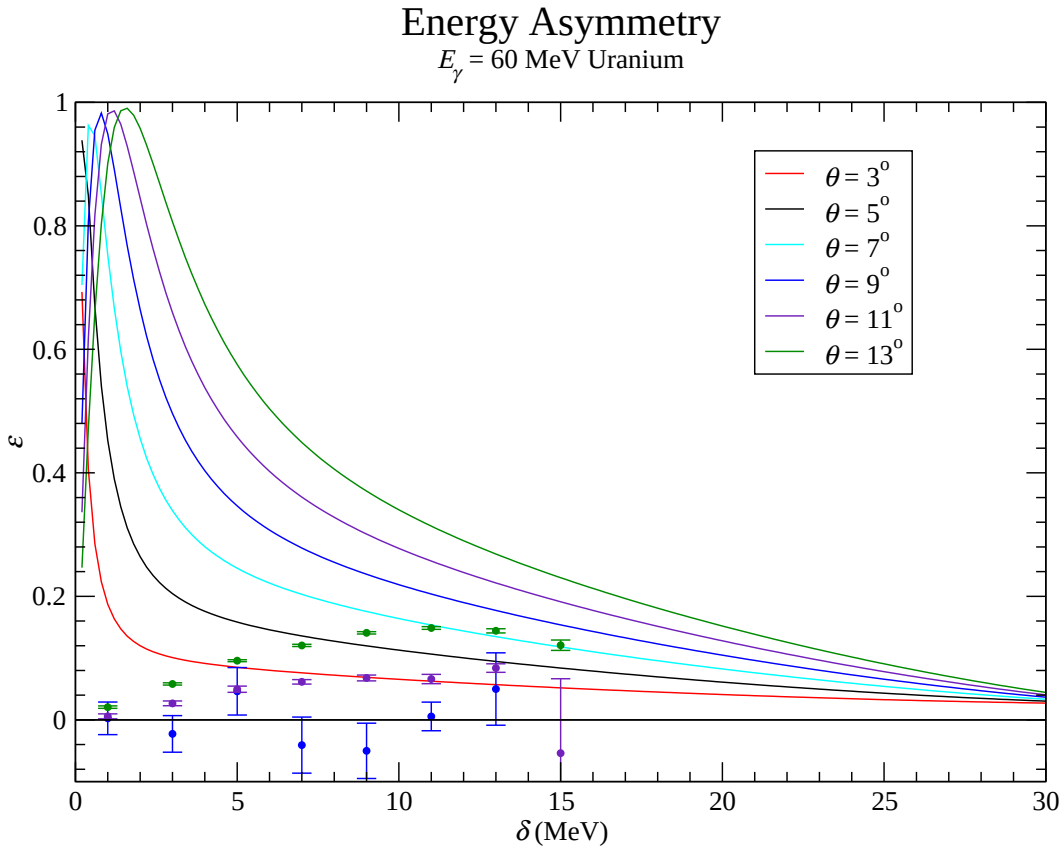

Figure 5: Measurable asymmetry with $\sigma_p = \sigma_q = 1.4$ MeV, $\sigma_\theta = 2.5°$, $\sigma_\phi = 7.8°$, $\Delta\theta_{tol} = 2.5°$, $\Delta\phi_{tol} = 8°$, $\Delta\theta_{bin} = 2°$ and $\Delta\delta_{bin} = 2$ MeV). 10^8 events that satisfied the criteria to fall within a bin were simulated. The simulation results for $\theta = 3°$, $5°$, and $7°$ are not shown since they are consistent with zero like the result for $\theta = 9°$.

7 Geant4 Simulation

We now attempt to generate events for direct input to the Geant4 simulation. The Geant4 simulation (described in SPIR-148) has been modified to allow input events to be read from a file rather than randomly generated at the beginning of each Geant4 event. This was necessary since the creation of events with a distribution defined by the differential cross section is a very time consuming process. This is because the cross section varies over many orders of magnitude as illustrated in figure 2. Allowing Geant4 to read events from a file allows he creation of that file to be done by multiple processes on multiple computers.

7.1 Using the full cross section

We first attempt to generate a set of events using the full acceptance of the spectrometer. We use to following procedure:

1. We choose an electron energy (K_p) in the range -20% to $+40\%$ of the spectrometer central energy $E_0 = 30$ MeV (the approximate acceptance).

2. We choose electron angles (θ_p and ϕ_p) and positron angles (θ_q and ϕ_q) that are uniform in phase space but restricted to angles within the acceptance of the spectrometer.

3. The positron energy (K_q) is then uniquely determined.

4. The differential cross section for this kinematics is calculated.

5. A random number is chosen and compared to the cross section to determine if this event is to be kept or not. If no, return to step 1.

6. If yes, the input parameters for the Geant4 code are calculated and written to a file.

Over 50,000 events were generated using this procedure (several CPU-weeks of computer time). The distribution of input events generated is shown in figures 6 and 7. Note that the "delta" in these plots is the percentage energy difference from the spectrometer central energy (not the electron/positron energy discussed above) and the "theta" and "phi" are the input angles at the target position as defined in figure 7 of SPIR-148 (not the polar and azimuthal angles).

The outputs of the Geant4 simulation are the positions and angles at the spectrometer detectors. These values are then used to calculate the energy and direction of the electron and positron emerging from the target using the fit to the spectrometer transfer matrix as described in Section 10 of SPIR-148.

The resulting electron-positron events are then tested for the kinematic condition required for the asymmetry requirement. Specifically we must satisfy Equation. (11)) with $\Delta\theta_{tol} = 2.5^\circ$ and $\Delta\phi_{tol} = 8^\circ$. Events that pass this test are then binned by polar angle (θ_i) and energy difference (δ_i) (Equation. (13)).

Finally, after processing all the events, the asymmetry (Equation. (14)) is calculated. This is shown in figure 8.

There are several things to note from this attempt.

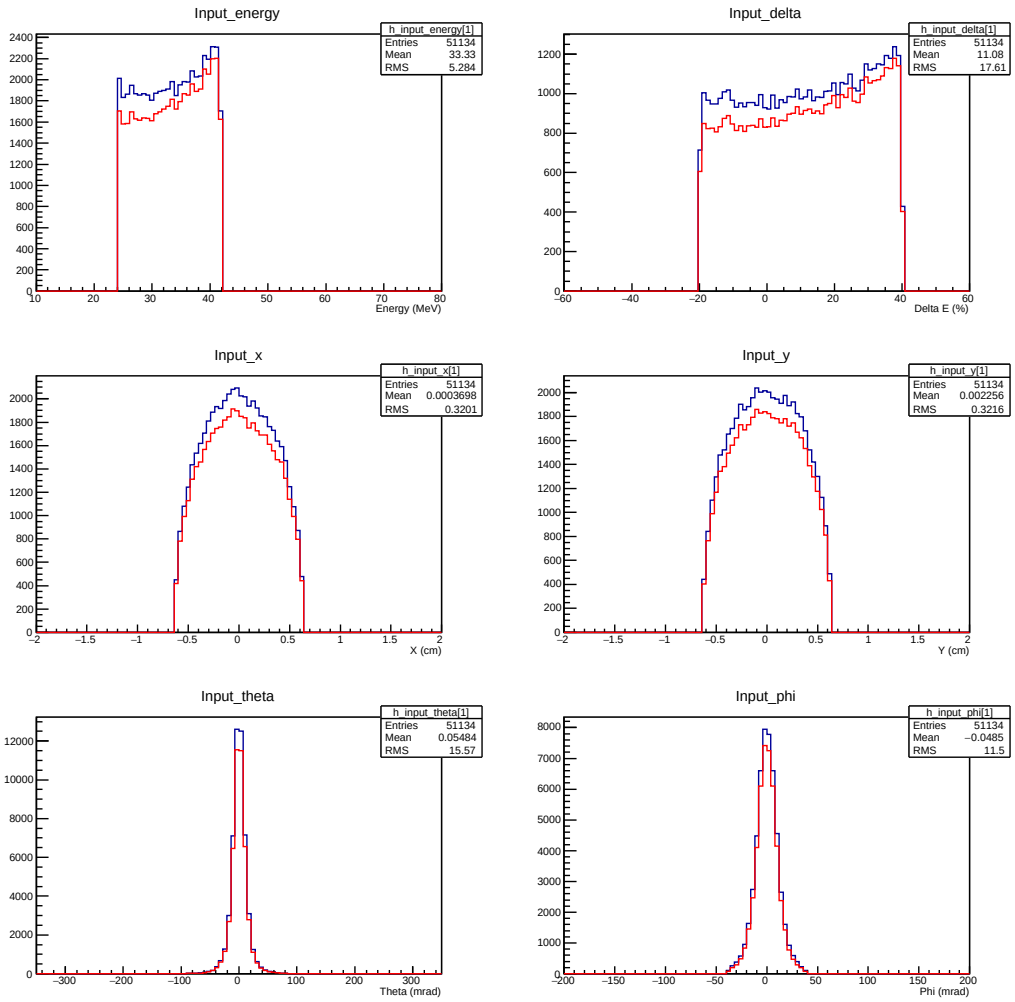

Figure 6: The electrons in the pair production events that are the input to the Geant4 simulation. The blue line shows the distribution of input electrons while the red line shows the distribution of those events that actually result in a hit on the appropriate detector after tracking through the spectrometer.

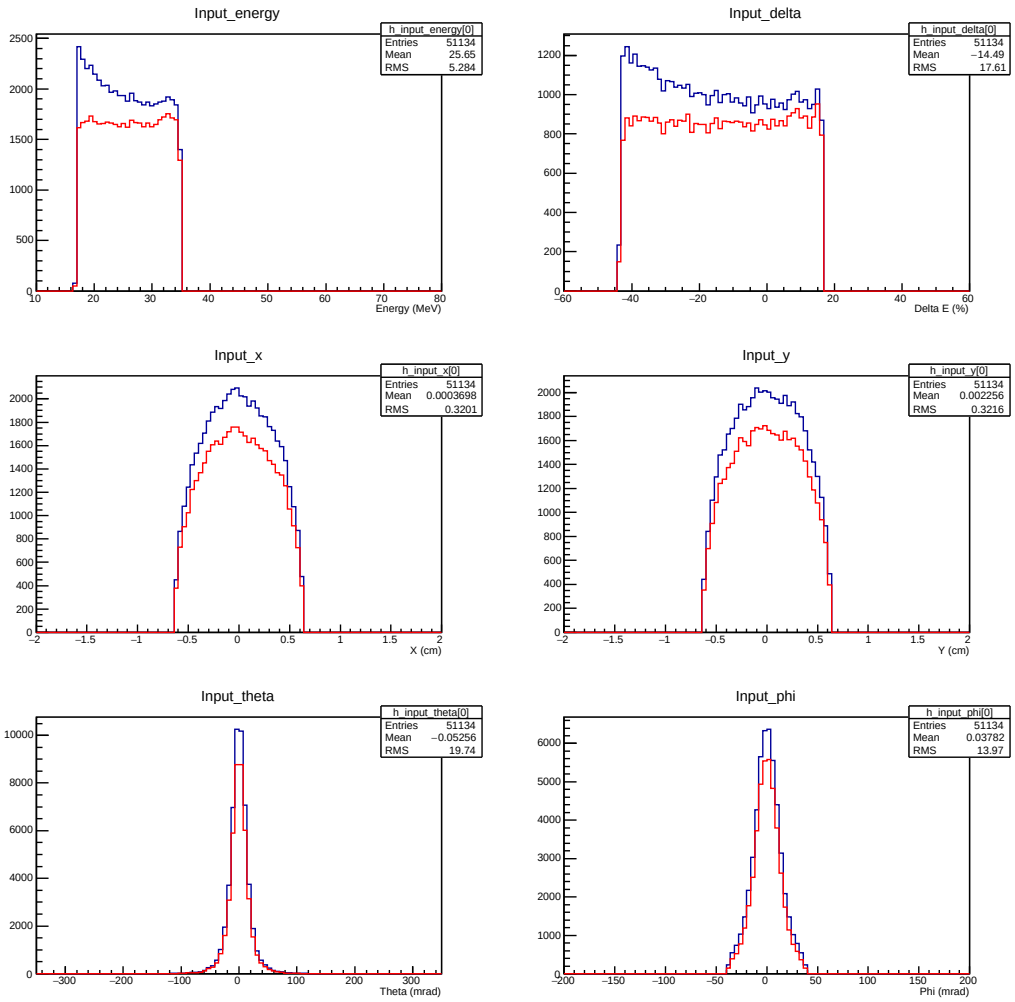

Figure 7: The positrons in the pair production events that are the input to the Geant4 simulation. The blue line shows the distribution of input electrons while the red line shows the distribution of those events that actually result in a hit on the appropriate detector after tracking through the spectrometer.

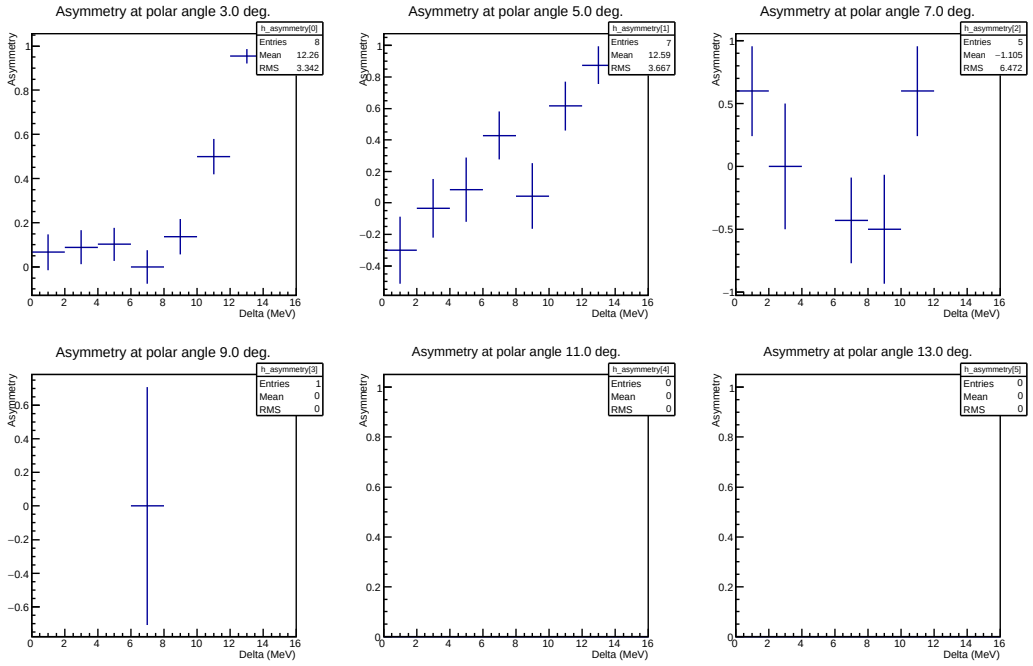

Figure 8: The asymmetry found from 51,000 events selected using the pair-production differential cross section and passed through the Geant4 simulation of the spectrometer.

Because the cross section falls very rapidly as a function of increasing polar angle most of the events generated are at very small polar angles ($< 5°$). Because of the limited angular resolution of the spectrometer it is not possible to accurately discriminate between events that satisfy the asymmetry kinematics condition. Therefore the asymmetries calculated for small polar angles are meaningless. This is consistent with what was found in section 6 above.

Because so few events fall at larger polar angle the asymmetries calculated there are also meaningless.

Finally, because in the generation of events, we first select electrons with energies within the approximate spectrometer acceptance, and therefore these are not distributed uniformly around the central energy of 30 MeV. The kinematics of pair production then in turn forces the distribution of positron energies to be oppositely non-uniform about the central energy. (See the "input_energy" plots in figures 6 and 7.) This introduces an asymmetry which may influence the final asymmetry calculated.

7.2 Using only large polar angles

To overcome the difficulties noted above we generate a new set of events for input to the Geant4 simulation. We use the same procedure as outlined in the previous section to select events except for the following two differences.

1. We choose the initial electron kinetic energy uniformly between -40% and $+40\%$ of

the spectrometer central energy. Hence the positron energies are also approximately uniformly distributed about the spectrometer central energy. We make this choice even though some of the events may be outside the acceptance of the spectrometer.

2. We do not generate any events that have either electron or positron polar angles less the 4°. Such events will be useless to us in the final analysis anyway because of the finite angular resolution of the spectrometer.

These choices very considerably speed up the process of generating events for input to the Geant4 simulation.

Shown below is the result for over 6 million generated events. The distribution of input events generated is shown in figures 9 and 10. Of those events, 2440146 of them result is valid hits on both the left and right pair spectrometer detectors and 1506760 events survive the kinematic condition required for the asymmetry requirement.

The resulting asymmetry plots are shown in figure 11. Because the input event are also included in the geant4 output we are able to calculate the asymmetry from the input values. These are shown in red in figure 11. These values should be the same as the values shown in figure 3 since the instrumental resolutions are set to zero and the bin widths used are the same. In general the comparison is good.

The blue points in figure 11 show the asymmetry from the events observed after tracking through the spectrometer and reconstructed to the target using the spectrometer transfer matrix.

The asymmetry at polar angles less than 7° are of course compromised by the choice to only use event with polar angles greater than 4°. As well the asymmetry at large values of the energy difference, $\delta > 12$ MeV, are influenced by the energy acceptance of the spectrometer. (This was the reason that we chose to only simulate events with energies $\pm 40\%$ of the central energy.) At other values the measured asymmetry should be similar to that calculated in the simple Monte-Carlo calculation and shown in figure 5. The comparison however is not good. The full simulation shows very small measurable asymmetry at polar angles greater than 11°. Only at the polar angles of 7° and 9° is the asymmetry statistically significant and have a measurable non-zero value.

As a check we can see how well the spectrometer transfer function is reproducing the energy and angle at the target. That comparison is shown in figures 12, 13 and 14 for the events in this simulation. We see that the transfer function is doing a good job. The energy, θ and ϕ difference distribution show the expected small widths. When these angle are translated into the polar and azimuthal angles we see that the distributions are larger. This is as predicted by the earlier simulations as described in SPIR-148[2]. It may be, that for the events that are of interest to us, these angular resolutions may not be good enough.

There is clearly more work to be done before we commit to running an experiment...

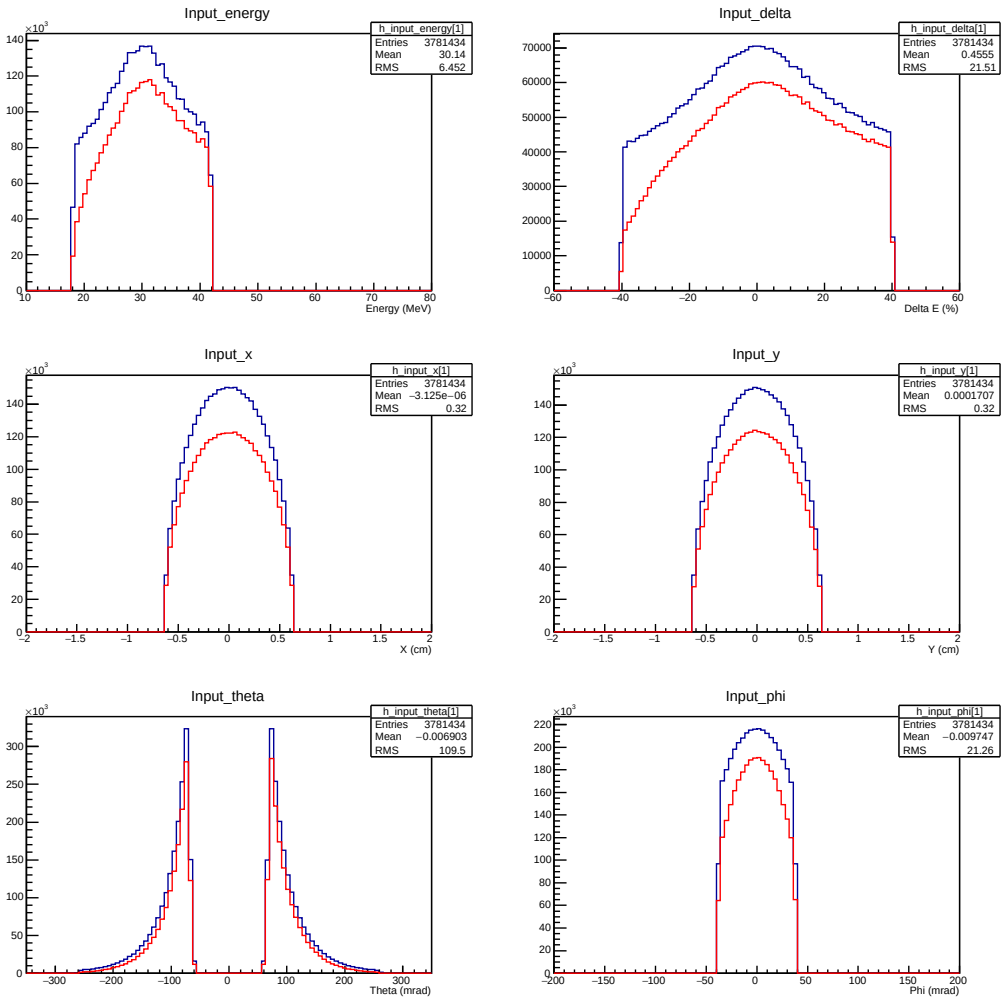

Figure 9: The electrons in the pair production events that are the input to the Geant4 simulation. In this simulation only events where both the electron and positron have polar angles greater than 4° are used. The blue line shows the distribution of input electrons while the red line shows the distribution of those events that actually result in a hit on the appropriate detector after tracking through the spectrometer.

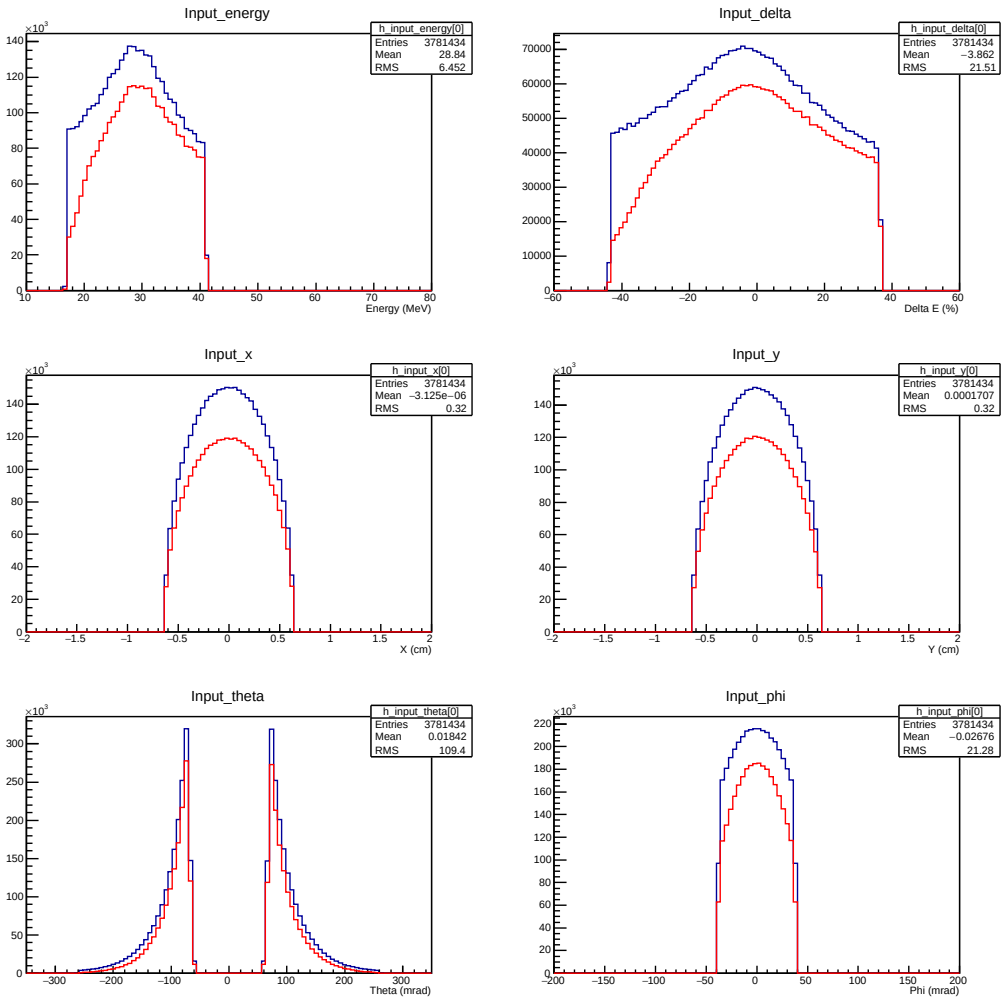

Figure 10: The positrons in the pair production events that are the input to the Geant4 simulation. In this simulation only events where both the electron and positron have polar angles greater than 4° are used. The blue line shows the distribution of input electrons while the red line shows the distribution of those events that actually result in a hit on the appropriate detector after tracking through the spectrometer.

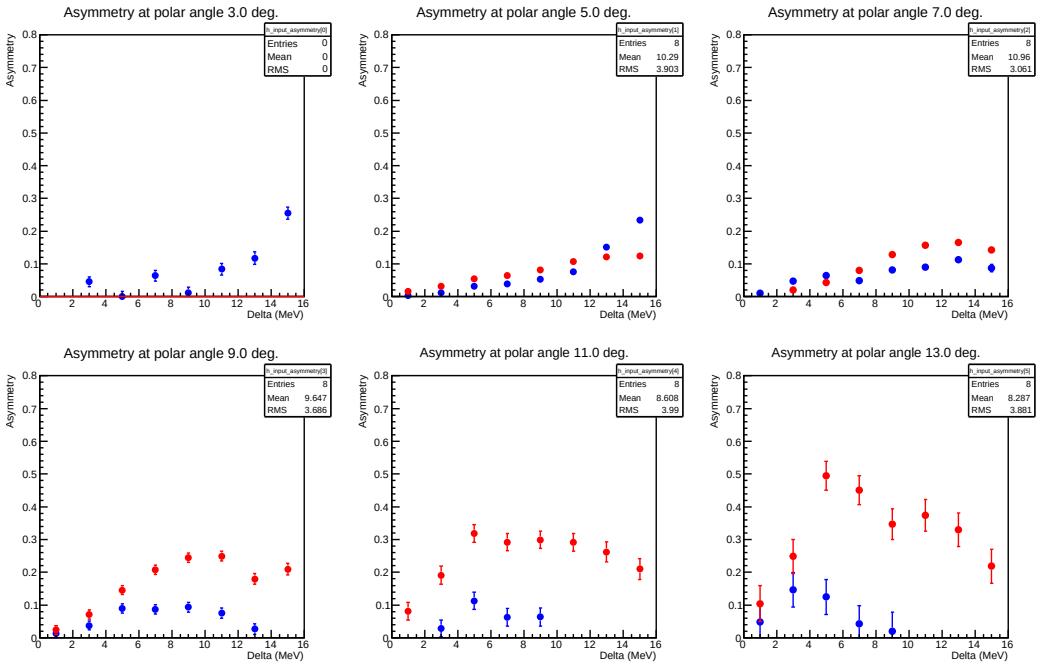

Figure 11: The asymmetry found from 6 million events selected using the pair-production differential cross section and passed through the Geant4 simulation of the spectrometer. Only events where the polar angle for both the electron and positron are greater than 4° are selected. The red points show the asymmetry calculated from the input values and the blue points are calculated from the reconstructed values from the spectrometer output.

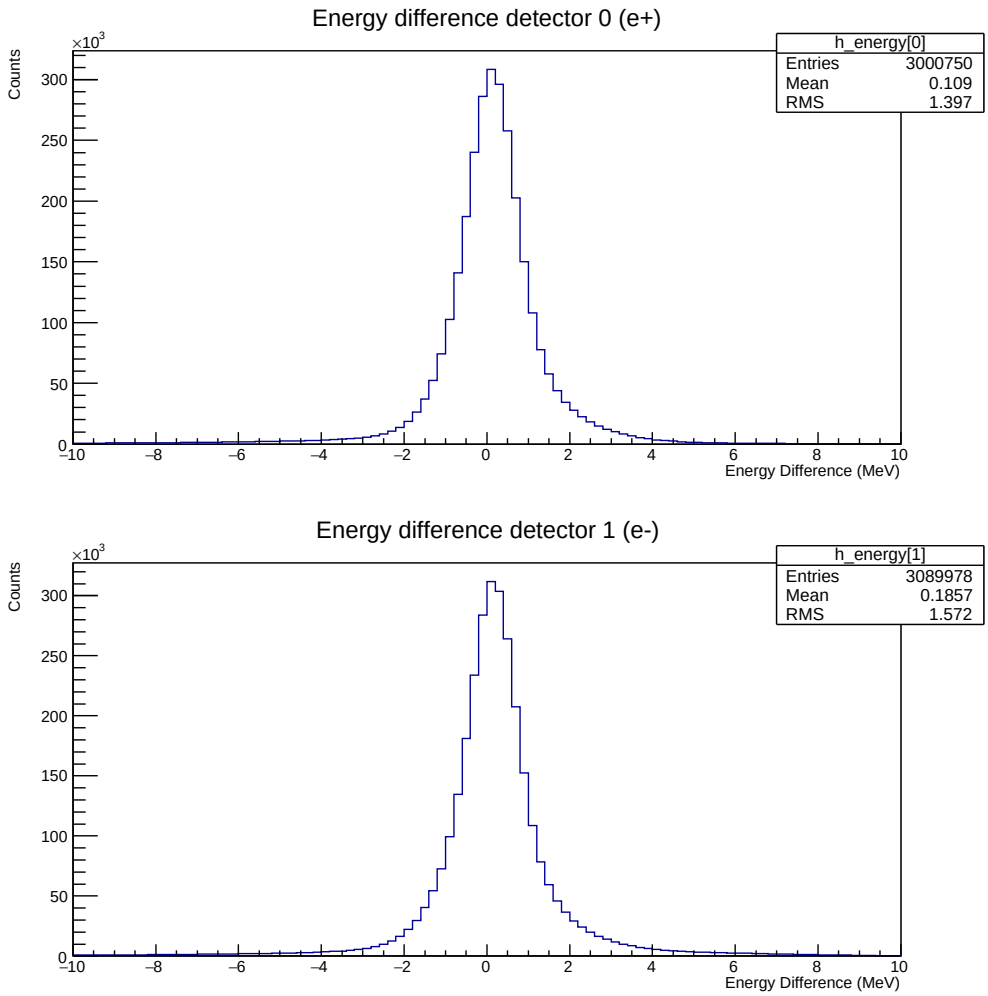

Figure 12: The difference between the reconstructed electron and positron energies at the target (using the spectrometer transfer function) and the input values.

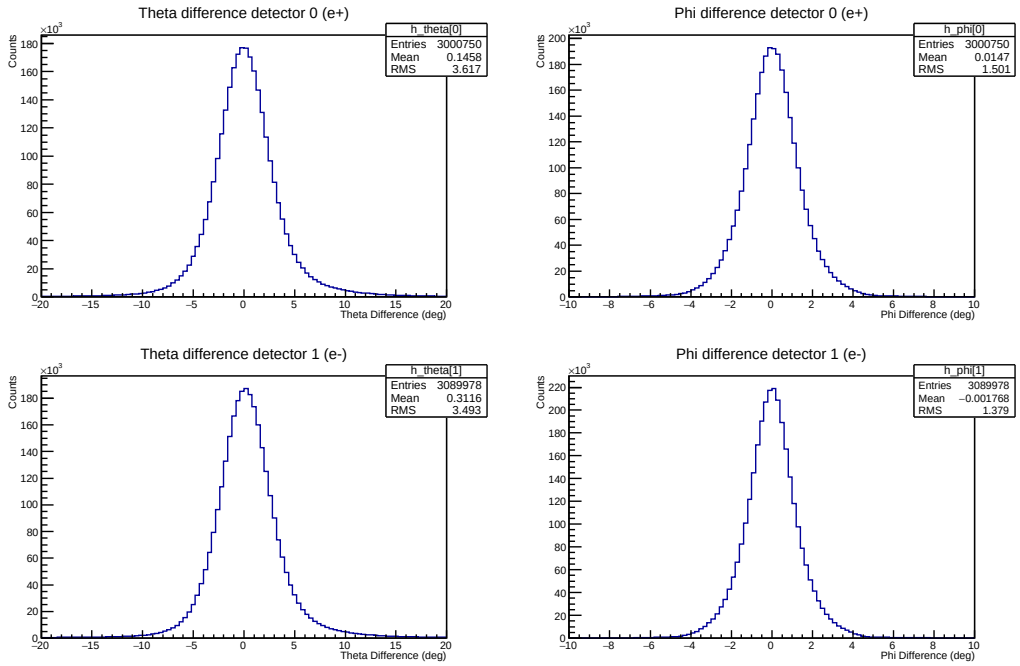

Figure 13: The difference between the reconstructed electron and positron θ and ϕ angles at the target (using the spectrometer transfer function) and the input values.

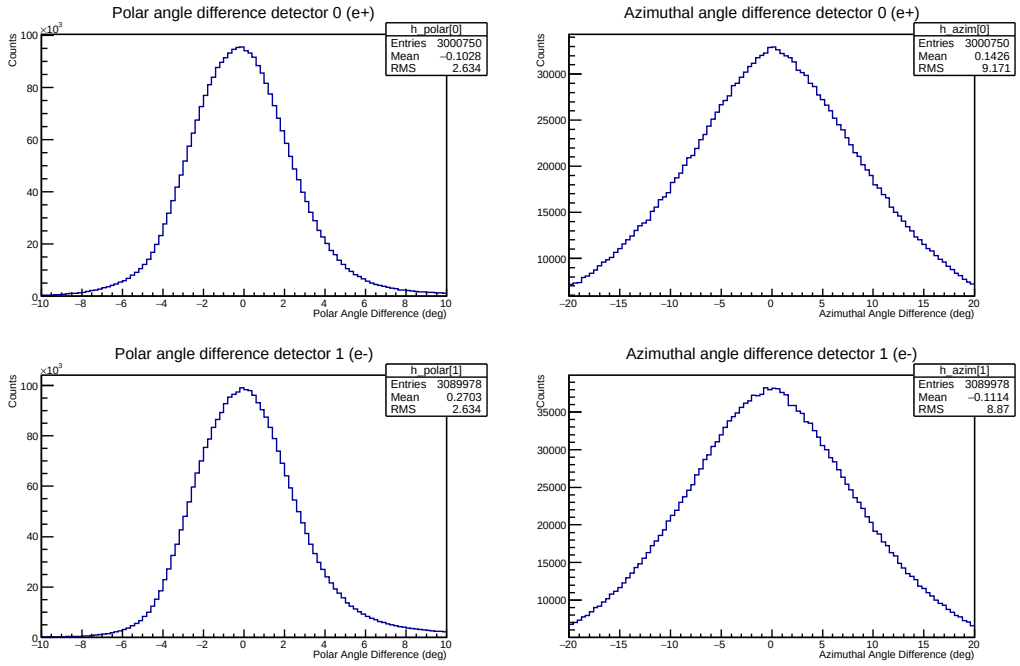

Figure 14: The difference between the reconstructed electron and positron polar and azimuthal angles at the target (using the spectrometer transfer function) and the input values.

A Error Calculations

To calculate the error in the asymmetry (Equation (5) or Equation (14)) we have an equation of the form

$$\epsilon = \frac{a-b}{a+b}.$$

The uncertainty $\delta\epsilon$ is related to the uncertainties δa and δb by

$$\delta\epsilon^2 = \left(\frac{\partial\epsilon}{\partial a}\right)^2 \delta a^2 + \left(\frac{\partial\epsilon}{\partial b}\right)^2 \delta b^2.$$

Then since

$$\left(\frac{\partial\epsilon}{\partial a}\right) = \frac{2b}{(a+b)^2} \text{ and } \left(\frac{\partial\epsilon}{\partial b}\right) = \frac{-2a}{(a+b)^2}$$

we get

$$\delta\epsilon^2 = \frac{4}{(a+b)^4}\left(b^2\delta a^2 + a^2\delta b^2\right),$$

and so

$$\delta\epsilon = \frac{2}{(a+b)^2}\left(b^2\delta a^2 + a^2\delta b^2\right)^{1/2}.$$

The calculation of the average cross section for falling in a particular bin follows from equation (15). The uncertainty in this number is calculated assuming that the distribution of the cross sections falling in a bin has a variance

$$\sigma_\sigma^2 = \frac{1}{N[\theta_i][\delta_j]}\left(\sigma_{sum}^2[\theta_i][\delta_j] - N[\theta_i][\delta_j]\bar{\sigma}[\theta_i][\delta_j]^2\right) \text{ with } \sigma_{sum}^2[\theta_i][\delta_j] = \sum_{k=0}^{N[\theta_i][\delta_j]} \sigma_k^2$$

where k runs over all events that fall within the bin.

The standard error in $\bar{\sigma}$ is then

$$\delta\bar{\sigma}[\theta_i][\delta_j] = \frac{\sigma_\sigma}{\sqrt{N[\theta_i][\delta_j]}}.$$

References

[1] G. Ron *et al.*, "A Measurement of the Bethe-Heitler Pair Production Asymmetries". Proposal to the HIGS PAC-12.

[2] Rob Pywell, Subatomic Physics Internal Report SPIR-148, "Bethe-Heitler Pair Spectrometer", University of Saskatchewan. (Available at `nucleus.usask.ca`)

[3] R.N. Lee, A.I. Milstein and V.M. Strakhovenko, "Charge asymmetry in the differential cross section of high-energy e^+e^- photo-production in the field of a heavy atom", Phys. Rev. A 85, 042104 (2012)